

## Proton Reaction Cross Sections and Strength Functions\*

A. J. ELWYN, A. MARINOV,† AND J. P. SCHIFFER

Argonne National Laboratory, Argonne, Illinois

(Received 5 January 1966)

The average yields of neutrons from proton-induced reactions in thick targets have been measured for about 33 elements in the mass region  $90 \leq A \leq 209$  at incident proton energies between 5.5 and 9.5 MeV. In this region of energies and masses, the  $(p,n)$  reaction overwhelms competing reactions so that, except in a few cases, the average  $(p,n)$  cross sections deduced from the measured yields are equal to the total reaction cross sections for protons. Reduced cross sections, which are directly related to the proton strength function, were obtained from the measurements. These results, as well as the results of previous measurements for  $A < 90$ , were compared with optical-model calculations. Proton reaction cross sections calculated from the optical potential of Perey are in remarkably good quantitative agreement with the measurements. The data are consistent with a resonance in the  $P$ -wave proton strength function at  $A \approx 105$ , and with dominant contributions from  $S$ - and  $D$ -wave protons at  $A \approx 65$  and for  $155 \leq A \leq 200$ . The measured angular distributions for some of the nuclei showed symmetry about  $90^\circ$  to about 2%, indicating no measurable direct-interaction component. The maximum anisotropy observed was about 7%.

### I. INTRODUCTION

THE proton strength function—the reduced proton width of nuclear resonance levels divided by the average energy spacing of the levels—is a quantity that is directly related to the average reaction cross section for protons. Furthermore, under certain circumstances the total reaction cross section for protons can be well approximated by the  $(p,n)$  reaction cross section. If, for example, the  $(p,n)$  reaction is performed at incident proton energies sufficiently below the Coulomb barrier for each target material, the emission of charged particles is inhibited and the compound nucleus decays almost entirely by neutron emission. The neutron yield integrated over all angles of emission is then a good approximation to the total reaction yield. Schiffer and Lee<sup>1</sup> have shown that under these circumstances the total neutron yield from thick targets bombarded by protons can be related to a “reduced cross section,” which is in turn directly related to the proton strength function. Presenting the data in this form has the advantage that the sharp energy and  $A$  dependence, which arises from the penetration of the Coulomb and centrifugal barriers, is removed and only variations caused by the nuclear interior remain.

In Ref. 1 it is shown that if  $\Gamma_p \ll \Gamma_n$  (where  $\Gamma_p$  is the incident proton width of the compound nuclear resonances, and  $\Gamma_n$  is the total neutron width for decay of resonance states), then on the basis of the Breit-Wigner resonance relation, and on the assumption of random resonant phases, the thick-target  $(p,n)$  reaction yield averaged over many resonances is given by

$$Y = \frac{\pi^2}{2I+1} \sum_{J,s,l} (2J+1) \frac{\langle \gamma_{J,s,l}^2 \rangle}{D_{J,s,l}} \int_{\Delta E} \frac{S\lambda}{A l^2} dE. \quad (1)$$

In Eq. (1),  $\langle \gamma_{J,s,l}^2 \rangle$  is the average reduced particle width

for levels of spin  $J$ , channel spin  $s$ , and relative orbital angular momentum  $l$ ;  $D_{J,s,l}$  is the level spacing,  $S$  is the stopping power of the target material in units of target atoms per  $\text{cm}^2$  MeV,  $2\pi\lambda$  is the wavelength of the incident proton,  $A l^2 = F l^2 + G l^2$  is inversely proportional to the usual Coulomb penetrability factor for the incident protons, and the integral is over the energy interval  $\Delta E$ . Equation (1) is obtained under the assumption that the level spacing is small compared with the energy required to make an appreciable change in  $S$ ,  $\lambda$ , and  $A l^2$ .

A reduced cross section  $\mathfrak{s}$  is defined by dividing the yield given in Eq. (1) by the weighted sum of the Coulomb penetrability factors. If we make the reasonable assumption that both  $\langle \gamma_{J,s,l}^2 \rangle$  and  $D_{J,s,l}$  are independent of channel spin, and the further assumption that the ratio  $\langle \gamma_{J,s,l}^2 \rangle / D_{J,s,l}$  is independent of  $J$ , then the reduced cross section becomes

$$\mathfrak{s} = \frac{\sum_l (2l+1) \langle \gamma_{J,s,l}^2 \rangle \int_{\Delta E} \frac{S\lambda}{A l^2} dE}{\sum_l (2l+1) \int_{\Delta E} \frac{S\lambda}{A l^2} dE}. \quad (2)$$

This expression represents an average of the strength function  $\langle \gamma_{J,s,l}^2 \rangle / D_{J,s,l}$ , the relative weights in the average being determined by the statistical and penetrability factors for each partial wave.

The optical model that describes the interaction of nucleons with nuclei predicts that resonances should occur in the total reaction cross section at energies corresponding to those of virtual single-particle states of the nucleon in the average nuclear potential. Since the reaction cross section is directly related to the strength function, peaks are predicted in the mass dependence of the nuclear strength functions. Most determinations of nuclear strength functions have been obtained through the study of neutron cross sections measured at low

\* Work performed under the auspices of the U. S. Atomic Energy Commission.

† Present address: The Hebrew University, Jerusalem, Israel.

<sup>1</sup> J. P. Schiffer and L. L. Lee, Jr., Phys. Rev. **109**, 2098 (1958).

energies. Experimental results<sup>2</sup> and theoretical interpretation<sup>3</sup> have established the existence of peaks in the  $S$ -wave neutron strength function at values of atomic weight  $A$  near 55 and 160 and in the  $P$ -wave strength function near  $A=95$ , and the possible existence of a  $D$ -wave peak at about  $A=140$ . In the mass region near  $A=160$ , the experimental values of the  $S$ -wave neutron strength function appear to fall on two peaks separated by about 40 mass units. As is well known, nuclides in this mass region are considerably deformed in their ground states; optical-model calculations with a spheroidal potential well<sup>4</sup> lead to two peaks in the strength function, in reasonable accord with the experimental results.

As with neutrons, the proton strength function is expected to show resonances as a function of atomic weight. Calculations by Margolis and Weisskopf,<sup>5</sup> for an intrinsic square-well proton potential plus a term to account for the Coulomb field, predict the existence of a peak in the  $S$ -wave strength function near  $A=68$ . Measurements by Schiffer and Lee<sup>1</sup> and by Johnson *et al.*<sup>6</sup> are in agreement with this prediction. Furthermore, the measurements indicate the possible existence of a peak in the  $D$ -wave strength function near  $A=50$ . Measurements by Almqvist *et al.*<sup>7</sup> of the total  $\gamma$ -ray yield following proton bombardment of nuclei also indicate that the proton reaction cross section is dominated by the  $S$ - and  $D$ -wave size resonances in the mass region  $50 \leq A \leq 70$ .

Both the experiments of Schiffer and Lee and those of Johnson *et al.* measured the yields of neutrons from  $(p,n)$  reactions on target materials from  $A=37$  to  $A=130$  by use of beams of incident protons with energies between 1 and 4 MeV accelerated in Van de Graaff generators. The purpose of the present study was to extend these measurements to elements of larger mass. To this end, a tandem Van de Graaff machine was employed to provide monoenergetic proton beams with

energies between 5.5 and 9.5 MeV. Measurements were performed on 33 targets having atomic weights between 90 and 209. For each element studied, the yields were determined at three values of the energy in the region corresponding to about 70% of the height of the Coulomb barrier. At energies much below this value, the fairly rapid variations of the proton penetrability factors as a function of energy might tend to overwhelm any resonance effects. Reduced cross sections were obtained from the measured yields, and the results were compared with optical-model calculations. Preliminary measurements of the neutron yields from  $(p,n)$  reactions on a number of nuclides in the present energy region have been reported by Schiffer and Jones.<sup>8</sup> A previous study of  $(p,n)$  reaction cross sections and their comparison with optical-model calculations on some nuclei up to  $A=120$  has been presented by Albert.<sup>9</sup>

## II. EXPERIMENT AND ANALYSIS

The monoenergetic proton beam from the Argonne tandem accelerator was incident on thick targets (about  $\frac{1}{8}$  in. in thickness) of the elements to be investigated in the form of self-supporting disks  $\frac{3}{4}$  in. in diameter. The disks (up to 18 elements at one time) were attached to a light Al frame; each target material could be lowered into the beam position under vacuum. The whole target assembly was fashioned from thin-walled Al pipe in an effort to minimize the effects of neutron interactions in the region around the targets. The proton beam was collimated onto the targets by two Ta apertures  $\frac{1}{8}$  in. in diam and about 10 in. apart, and placed 3 ft from the target. The whole target assembly served as a Faraday cup by which proton charge was measured through the use of a current integrator.

Neutrons produced in the  $(p,n)$  reaction were detected by a long counter set at a distance of  $30\frac{1}{4}$  in. from the target position. The efficiency of the long counter was calibrated by use of a  $\text{Cf}^{252}$  neutron source of known intensity.<sup>10</sup> The energy spectrum of the neutrons emitted from a fission source such as  $\text{Cf}^{252}$  has approximately the same shape as is expected for the neutrons emitted from proton bombardment of a heavy nucleus; they are both "evaporation" spectra from highly excited compound nuclei. It is advantageous, therefore, to use such a source for calibration purposes in the present experiment. Measurements of the yields were made at an angle of  $90^\circ$  with respect to the incident proton beam. The targets were oriented so that the normals to the  $\frac{3}{4}$ -in.-diam planes made an angle of  $45^\circ$  with respect to the proton beam. The yields were measured first in transmission and then in reflection; and these counting rates were averaged to obtain the final results. It was

<sup>2</sup> D. J. Hughes, R. L. Zimmerman, and R. E. Chrien, *Phys. Rev. Letters* **1**, 461 (1958); R. E. Coté, L. M. Bollinger, and J. M. LeBlanc, *Phys. Rev.* **111**, 288 (1958); J. M. LeBlanc, R. E. Coté, and L. M. Bollinger, *Nucl. Phys.* **14**, 120 (1959); L. W. Weston, K. K. Seth, E. G. Bilpuch, and H. W. Newson, *Ann. Phys. (N. Y.)* **10**, 477 (1960); A. Saplakoglu, L. M. Bollinger, and R. E. Coté, *Phys. Rev.* **109**, 1258 (1958); J. P. Desjardins, J. L. Rosen, W. W. Havens, Jr., and J. Rainwater, *ibid.* **120**, 2214 (1960); K. K. Seth, R. H. Tabony, E. G. Bilpuch, and H. W. Newson, *Phys. Letters* **13**, 70 (1964).

<sup>3</sup> H. Feshbach, C. E. Porter, and V. F. Weisskopf, *Phys. Rev.* **96**, 448 (1954); H. Fiedeldey and W. E. Frahn, *Ann. Phys. (N. Y.)* **19**, 428 (1962); *Nucl. Phys.* **38**, 686 (1962); B. Buck and F. Perey, *Phys. Rev. Letters* **8**, 444 (1962); P. A. Moldauer, *Nucl. Phys.* **47**, 65 (1963).

<sup>4</sup> F. S. Troubetskoj and B. Margolis, *Phys. Rev.* **106**, 105 (1956); D. M. Chase, L. Wilets, and A. R. Edmonds, *ibid.* **110**, 1080 (1958).

<sup>5</sup> B. Margolis and V. F. Weisskopf, *Phys. Rev.* **107**, 641 (1957).

<sup>6</sup> C. H. Johnson, A. Galonsky, and J. P. Ulrich, *Phys. Rev.* **109**, 1243 (1958).

<sup>7</sup> E. A. Almqvist, D. A. Bromley, J. A. Kuehner, and E. W. Vogt, in *Proceedings of the International Conference on Nuclear Structure, Kingston, Canada, 1960*, edited by D. A. Bromley and E. W. Vogt (North-Holland Publishing Co., Amsterdam, 1960), p. 736.

<sup>8</sup> J. P. Schiffer and G. A. Jones, in *Proceedings of the International Conference on Nuclear Structure, Kingston, Canada, 1960*, edited by D. A. Bromley and E. W. Vogt (North-Holland Publishing Co., Amsterdam, 1960), p. 676.

<sup>9</sup> R. D. Albert, *Phys. Rev.* **115**, 925 (1959).

<sup>10</sup> We wish to thank Dr. H. Diamond of Argonne National Laboratory for providing us with the  $\text{Cf}^{252}$  source.

found that this method of obtaining data accounts, at least approximately, for the effects of neutron scattering and absorption in the thick targets that were utilized.<sup>11</sup>

The number of background neutrons that are detected was small in the present experimental arrangement. Most such neutrons originate in the region of the Ta collimators, which are 3 ft away from the targets of interest and even farther from the long counter. Under normal operating conditions, these background neutron events amounted to less than 1% of the total number of neutrons counted for any given target material.

A number of angular distributions were measured to check on the absence of direct-interaction effects, as well as to test the reliability of the use of the 90° yield as a measure of the total ( $p,n$ ) cross section. In all cases the angular distributions were symmetric about 90° to within 2%, and were almost isotropic; the maximum anisotropy was about 7%. These results are in approximate agreement with the statistical theory of Hauser and Feshbach,<sup>12</sup> in which symmetry about 90° is predicted for the outgoing particles, and which further predicts isotropy if many levels (in a statistical sense) in the final nucleus are excited. Since the 90° yield served as a measure of the total ( $p,n$ ) cross section, the lack of isotropy in the present results leads to measured total ( $p,n$ ) cross sections that are perhaps 3–4% too low.

Measurements were made on targets having the natural isotopic abundances. In most cases (except for a few of the elements with atomic weights between ~90 and 100) the measured ( $p,n$ ) yield represents an average of the yields of all of the stable isotopes. In all, about 33 elements, with atomic weights between 90 and 209, were studied.

The experiment was performed at three energies for each of the target materials; the highest energy was at a value corresponding to about 70% of the height of the Coulomb barrier for each element. The range of energy was from 5.5 to 9.5 MeV. For most cases, the proton penetrability factors had values less than 10% of the values of the corresponding neutron penetrabilities. Nonetheless, in some cases (notably near  $A=90$ ), the proton penetrability was larger than 10% of the neutron values. In most of these latter cases, however, the ( $p,n$ ) reaction in question involved a stable isotope that was not the dominant isotope in the target material. If the average neutron and proton reduced widths are equal, the assumption  $\Gamma_p \ll \Gamma_n$  is thought to be quite good for

all but a few of the levels excited in the ( $p,n$ ) reactions studied in the present work. The emission of neutrons, therefore, dominates possible charged-particle decay of the compound system for most cases. For some of the target materials, in particular Ta, Re, Ir, Au, and Tl, the ( $p,2n$ ) reaction is energetically allowed within the energy range at which each of these elements was studied, and might compete with the ( $p,n$ ) reaction. The final measured results show, however, that this is not the case, at least not in a completely consistent fashion. The effect of the ( $p,2n$ ) reaction on the measured yield, therefore, is thought to be negligibly small; in particular, it is most unlikely to affect conclusions based on the systematic behavior of the present results.

The average neutron counting rate for a given accumulation of proton charge was converted to neutron yield per incident proton. These results are shown for the various target materials and bombarding energies in column 3 Table I. Column 4 lists the mean ( $p,n$ ) cross sections (in mb MeV) for the element in question. These were obtained from the neutron yields in column 3 by use of the effective stopping power for the target at the energies indicated. Reduced cross sections, defined in Eq. (2), were obtained by dividing the measured yields (corrected for chemical and isotopic abundances where necessary) by the quantity in the denominator of Eq. (2). These are shown in column 5 of the table. Since the values of  $S$  showed no systematic variation with bombarding energy, the three values for each element were averaged to obtain the results given in the last column of the table. The errors shown for these average values are the relative errors associated with the measured cross sections. The absolute errors on the values of the average reduced cross section are estimated to be about 20–25%.

The determination of the reduced cross section involves the evaluation of the integral shown in the denominator of Eq. (2). This was accomplished by the use of improved versions of the computer programs discussed in Ref. 1. The quantity

$$\sum_l (2l+1) \int_{\Delta E} \frac{\lambda}{A l^2} dE$$

was evaluated and then multiplied by values of the stopping power  $S$ , suitably averaged over the energy interval  $\Delta E$ . The values of stopping power were obtained from the compilation of Williamson and Boujot<sup>13</sup> either directly or by interpolation. For the penetrability calculation, a radius of  $R=1.45A^{1/3}$  F was employed.

In order to evaluate the above-mentioned integral, it is necessary to know the  $Q$  values for ( $p,n$ ) reactions on the various stable isotopes of the elements studied. In practically all cases, the values used are consistent with

<sup>11</sup> The effect of the thickness of the targets on the counting rates of the neutrons produced in the ( $p,n$ ) reaction was investigated in the following manner. A thin Ta foil (just thick enough to stop all of the incident protons) was placed directly in front of the thick disk of the target material of interest, and the counting rate was determined in reflection. The difference between this rate and the rate for a thin Ta foil alone is a measure of target-thickness effects on neutron counting rates. In all cases tested, the resultant counting rate, obtained by subtracting this difference from the measured rate for the target element alone (in reflection), agreed to within 2% with the average of the rates in transmission and reflection.

<sup>12</sup> W. Hauser and H. Feshbach, Phys. Rev. **87**, 366 (1952).

<sup>13</sup> C. Williamson and J. P. Boujot, CEA Report No. 2189, Centre d'etudes Nucleaires de Saclay, France, 1962 (unpublished).

TABLE I. Summary of measurements.

Target	Bombarding energy (MeV)	Neutrons per incident proton ( $10^{-7}$ )	$\bar{\sigma}$ (mb)	$S$ ( $10^{-14}$ cm)	$\langle S \rangle$ ( $10^{-14}$ cm)	Target	Bombarding energy (MeV)	Neutrons per incident proton ( $10^{-7}$ )	$\bar{\sigma}$ (mb)	$S$ ( $10^{-14}$ cm)	$\langle S \rangle$ ( $10^{-14}$ cm)
Zr	5.5	79.2	95.2	6.88	7.03±0.54	Gd	7.0	52.4	35.3	7.32	7.37±0.53
	6.0	155.4	175.1	7.19			7.5	105.9	68.0	7.34	
Nb	6.0	239.8	132.9	6.25	6.46±0.71		8.0	198.7	122.0	7.47	
	6.5	439.3	229.6	6.66		Tb	7.0	43.8	29.6	7.09	7.18±0.52
Mo	5.5	98.1	59.8	7.22	7.29±0.73		7.5	91.1	58.8	7.21	
	6.0	209.3	119.8	7.54			8.0	170.8	105.4	7.24	
	6.5	361.8	195.2	7.10		Dy	7.0	38.7	26.6	7.11	7.10±0.64
Rh	5.5	77.2	48.8	7.32	7.46±0.59		7.5	80.2	52.6	7.12	
	6.0	162.7	96.6	7.39			8.0	150.2	94.1	7.06	
	6.5	319.0	178.8	7.69		Ho	7.0	32.5	22.5	6.88	6.99±0.52
Pd	5.5	59.7	38.8	7.04	7.35±0.69		7.5	68.9	45.6	6.96	
	6.0	135.4	82.6	7.31			8.0	135.2	85.5	7.14	
	6.5	271.8	156.6	7.69		Er	7.5	64.8	43.2	7.45	7.16±0.76
Ag	5.5	54.7	35.6	7.17	7.35±0.60		8.0	123.4	78.6	7.33	
	6.0	120.2	73.6	7.29			8.5	201.7	123.3	6.71	
	6.5	240.3	138.8	7.59		Tm	7.5	54.5	36.5	7.20	6.93±0.76
Cd	5.5	44.2	29.6	7.01	7.27±0.65		8.0	106.2	67.9	7.14	
	6.0	102.0	64.2	7.24			8.5	173.2	106.3	6.45	
	6.5	210.5	125.0	7.57		Yb	7.5	46.6	31.7	6.90	6.81±0.59
In	6.0	90.2	57.2	7.17	7.42±0.60		8.0	93.9	61.2	7.01	
	6.5	188.7	112.9	7.51			8.5	159.7	99.7	6.53	
	7.0	346.2	196.4	7.57		Ta	8.0	59.6	39.8	6.36	6.70±0.68
Sn	6.5	154.6	94.5	7.27	7.47±0.60		8.5	117.5	75.3	6.64	
	7.0	295.6	174.2	7.68			9.0	220.7	136.0	7.13	
Sb	6.0	71.2	46.5	7.37	7.52±0.60	W	8.0	56.3	38.0	6.78	6.54±0.56
	6.5	150.3	92.9	7.60			8.5	100.3	65.0	6.31	
	7.0	276.9	162.2	7.59			9.0	183.5	114.3	6.53	
Te	6.0	63.9	43.2	7.44	7.49±0.53	Re	8.0	50.1	34.0	6.81	7.24±0.82
	6.5	134.4	85.8	7.52			8.5	101.9	66.5	7.18	
	7.0	250.7	151.8	7.51			9.0	195.6	122.7	7.72	
CsI	7.0	174.8	104.8	6.71	6.76±0.48	Ir	8.0	38.6	26.9	6.67	7.13±0.83
	7.5	311.2	177.6	6.80			8.5	81.3	54.4	7.13	
Ba	6.5	57.9	37.6	5.51	5.53±0.49		9.0	158.1	101.6	7.61	
	7.0	115.4	71.1	5.53		Pt	8.0	33.2	23.2	6.50	6.66±0.51
	7.5	209.2	122.7	5.55			8.5	68.2	45.8	6.70	
La	6.5	56.3	36.7	6.24	6.11±0.57		9.0	127.5	82.3	6.78	
	7.0	110.8	68.6	6.09		Au	8.0	27.6	19.4	6.16	6.37±0.54
	7.5	200.8	118.5	6.02			8.5	57.3	38.6	6.36	
Pr	6.5	44.1	28.9	6.76	6.40±0.75		9.0	110.8	71.9	6.59	
	7.0	86.3	53.6	6.35		Tl	8.5	50.1	34.4	6.82	7.22±0.76
	7.5	156.9	92.9	6.10			9.0	100.4	66.4	7.21	
Nd	6.5	31.9	21.2	5.94	6.04±0.56		9.5	187.6	119.6	7.62	
	7.0	70.5	44.6	6.04		Pb	8.5	45.9	31.7	7.00	7.07±0.50
	7.5	139.4	84.0	6.16			9.0	89.2	59.3	7.09	
Sm	7.0	60.8	39.6	6.59	6.60±0.59		9.5	159.3	102.0	7.11	
	7.5	120.2	74.7	6.57		Bi	8.5	40.4	28.0	6.99	7.07±0.51
	8.0	217.0	128.8	6.63			9.0	79.1	52.7	7.06	
							9.5	144.4	92.7	7.15	

those given in the recent compilation of Mattauch *et al.*<sup>14</sup> In those cases for which  $Q$  values are not known (mostly for isotopes which were only a few percent abundant), reasonable estimates were employed. Moreover, since most of the measurements were performed far above the threshold energies, relatively large errors in  $Q$  values could be tolerated.

### III. DISCUSSION

The optical model has been reasonably successful in accounting for many of the observed features in the elastic scattering of protons by nuclei. In the case of

<sup>14</sup> J. H. E. Mattauch, W. Thiele, and A. H. Wapstra, Nucl. Phys. **67**, 32 (1965).

proton reaction cross sections, systematic data available for analysis are much less abundant. In Fig. 1 the measured energy-averaged ( $p,n$ ) cross sections (from column 4, Table I) are compared with optical-model calculations of the cross section for compound nucleus formation. The calculations (the smooth curves in Fig. 1) are based on the surface-absorption optical potential given by Perey,<sup>15</sup> who obtained the values of the parameters of the model from an extensive systematic analysis of proton elastic-scattering data in the energy

<sup>15</sup> F. G. Perey, Phys. Rev. **131**, 745 (1963). In the notation of this reference, the values of the parameters are  $V_s = 53.3 - 0.55E + 0.4Z/A^{1/3} + 27(N-Z)/A$ ,  $W_D = 12$  MeV,  $r_{0s} = 1.25$  F,  $a_s = 0.65$  F,  $r_{0I} = 1.25$  F,  $a_I = 0.47$  F,  $V_{so} = 7.5$  MeV.

range between 9 and 22 MeV. The real well depth of the model is energy dependent, and also contains a term dependent on the nuclear symmetry number  $(N-Z)/A$ ; the other parameters are taken to be independent of energy.<sup>15</sup> The agreement between the calculations and the present experimental results is best in the mass regions  $100 \lesssim A \lesssim 150$  and  $180 \lesssim A \lesssim 195$ . From  $A \approx 150$  to  $A \approx 180$ , the region of strongly deformed nuclei, the agreement between measured cross sections and calculations based on a spherical optical model is less good—as might be expected.

The mean reduced cross sections (column 6, Table I) are plotted in Fig. 2 as a function of atomic weight  $A$ . Also shown in the figure are most of the earlier measurements of Schiffer and Lee,<sup>1</sup> who studied elements between  $A=37$  and  $A=130$  at proton bombarding energies between 2 and 4 MeV. These earlier results have been re-analyzed by use of techniques consistent with those employed for the present series of measurements. As can be seen, there is good agreement in the region  $90 \leq A \leq 130$ —the region in which the two experiments overlap. The reduced cross sections of Ref. 1 showed no systematic variation with energy; this behavior is consistent with the results of the present series of measurements. For those nuclei common to the two experiments, therefore, the reduced cross section exhibits no systematic energy dependence in the range from about 3.5 to 6.5 MeV.

The smooth curve in Fig. 2 is the result of an optical-model computation in which the calculated compound-nucleus cross sections integrated over energy were divided by the expression in the denominator of Eq. (2). The model potential used is the one described in the previous paragraphs. Although some of the actual details in the data are not reproduced by the calculations, the disagreement between calculations and measurements is not worse than 10–15%, at least in the region of  $A \geq 90$ .

In particular, for  $90 \leq A \leq 144$  the comparison is excellent. The 25% fall-off in the measured reduced cross

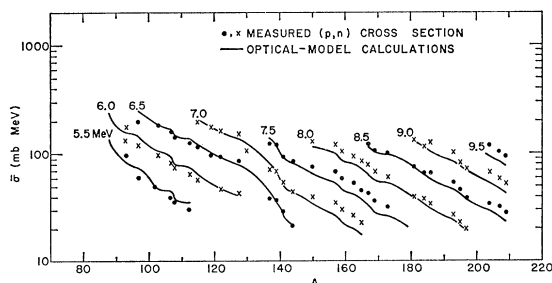


FIG. 1. The cross sections (at each of the indicated incident-proton energies) as a function of the atomic weight  $A$ . The points (circles and  $\times$ 's) are measured energy-averaged  $(p,n)$  reaction cross sections. The compound-nucleus cross sections (curves) were calculated on the basis of the optical model of Ref. 15 by use of the ABACUS 2 computer code of E. H. Auerbach [Brookhaven National Laboratory Report BNL-6562, 1962 (unpublished)].

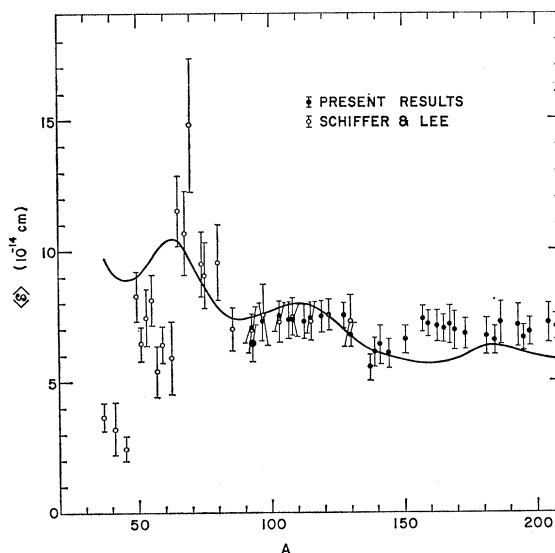


FIG. 2. The mean reduced cross sections (Ref. 1 and column 6 of Table I) as a function of  $A$  (points) compared with calculations (curves) based on the optical model of Ref. 15. The calculated curves result from dividing the computed compound-nucleus cross sections integrated over energy by the weighted sum of the Coulomb penetrability factors [the denominator of Eq. (2)].

sections between  $A=127$  and  $138$  is well fitted by the calculations, although the decrease is perhaps more gradual than the fall-off in the measured results. For the values of atomic weight covered in the present experiment, the poorest agreement between calculated and measured results is found for  $A$  between 145 and 180. As mentioned, this is a mass region in which many of the nuclides are strongly deformed. It is not unreasonable, therefore, that the measurements should disagree with calculations based on a spherical optical model.

For nuclides with  $A < 80$ , the data (the results of Ref. 1) fall on two peaks lying at  $A \approx 50$  and  $A \approx 68$ . The calculations, however, show a single resonance with a peak near  $A = 65$ . The very low measured values for  $\langle \sigma \rangle$  associated with the nuclei  $\text{Cl}^{37}$ ,  $\text{K}^{41}$ , and  $\text{Sc}^{45}$  have been discussed in Ref. 1. Corrections that take account of the possibility of  $(p,\alpha)$  reactions on these target elements<sup>16</sup> tend to raise these low values into reasonable agreement with nearby nuclides.<sup>1</sup>

A more detailed understanding of the results can be obtained by decomposing the optical-model calculations into their partial-wave components. The relative contribution to the yield of incident protons with different  $l$  values is shown in Fig. 3, in which the optical-model compound-nucleus cross sections (for the  $l$  values shown) have been plotted as a function of atomic weight. Further, in Fig. 4 the proton strength function determined by dividing the optical-model transmission coefficients by the Coulomb penetrability factors is plotted as a function of  $A$ . The values plotted in Figs. 3

<sup>16</sup> R. L. Clarke, E. A. Almquist, and E. B. Paul, Nucl. Phys. **14**, 472 (1959).

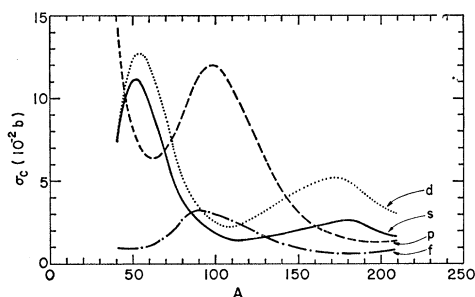


FIG. 3. The calculated relative contributions to the yield of the incident protons with different values of  $l$  as a function of atomic weight  $A$ . The values are plotted for the approximate region of bombarding energies used. These calculations were based on the optical model of Ref. 15.

and 4 were calculated for the approximate region of bombarding energies used in the experiment.

On the basis of these results, one can conjecture about the origin of the structure observed in the plot (Fig. 2) of the average reduced cross section versus  $A$ . It is clear, for example, that the fall-off in the reduced cross sections from  $A=120$  to  $140$  can be associated with a large decrease in the  $P$ -wave transmission coefficients.

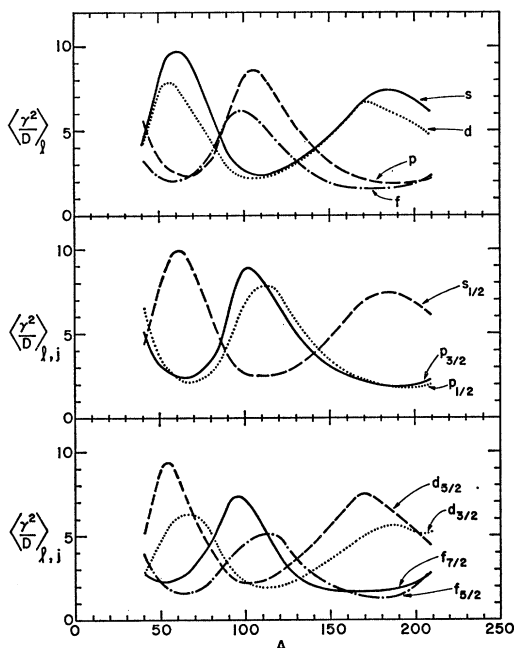


FIG. 4. The calculated proton strength function (arbitrary units) for various values of  $(l, j)$  (the two lower sets of curves) and for values of  $l$  (the upper sets of curves) as a function of atomic weight  $A$ . The strength functions are plotted for the approximate region of bombarding energy used. The values were determined by dividing the optical-model transmission coefficients by the Coulomb penetrability factors.

The measurements are, therefore, consistent with a peak in the  $P$ -wave proton strength function at  $A \approx 105$ . At higher atomic weights, the calculations indicate that  $S$ - and  $D$ -wave proton capture is predominant. The measurements for values of  $A$  from 155 to 209 show a systematic tendency to lie on two peaks separated by some 35 mass units, although the evidence for such behavior is not completely unambiguous. The situation is, however, similar to the experimental situation for the neutron strength functions in this mass region, for which optical-model calculations that employed a spheroidal potential well predicted the splitting of the  $S$ -wave strength-function resonance into two peaks in approximate agreement with experiment.<sup>4</sup> It is likely, therefore, that specific properties of deformed nuclei also play an important role for the proton strength function for  $A \geq 155$ .

In the region of atomic weight  $A < 80$ , it is reasonable to assume—on the basis of Figs. 3 and 4—that the peaks in the reduced cross sections (Fig. 2) can be associated with both  $S$ - and  $D$ -wave proton capture. This is in approximate agreement with the earlier conclusions of Schiffer and Lee,<sup>1</sup> who identified the measured peak at  $A \approx 50$  with a resonance in the  $D$ -wave proton strength function, and the peak at  $A \approx 68$  with the  $S$ -wave strength function. For these lighter nuclei the known isobaric-spin splitting of the proton single-particle states could be a partial explanation of the differences between calculated and measured cross sections. Such effects are not explicitly included in the optical model and for nuclei with  $(N-Z) \leq 4$  they may be important. In the heavier nuclei with  $(N-Z) \geq 6$  the neglect of this splitting is probably unimportant.

The conclusions of the present work—that the  $P$ -wave proton strength function peaks at  $A \approx 105$ , and that  $S$ - and  $D$ -wave strength functions dominate near  $A \approx 65$  and for  $155 \leq A \leq 200$ —have been based on a particular optical model. This model,<sup>15</sup> which is consistent with a large amount of proton scattering data, has also been shown to be in reasonable agreement with some neutron scattering results. For example, Wilmore and Hodgson<sup>17</sup> have compared measured differential cross sections for 1–14-MeV neutrons scattered from a number of nuclei with calculations based on a potential corresponding to the proton optical model of Perey, and have found good agreement between calculated and measured results.

#### ACKNOWLEDGMENTS

We would like to thank Dr. J. E. Monahan for helpful discussions, and W. Ray, J. Wallace, W. Evans, and the crew of the Argonne tandem accelerator for their assistance with the experiment.

<sup>17</sup> D. Wilmore and P. E. Hodgson, Nucl. Phys. **55**, 673 (1964).